Modelling macrosegregation in a 2.45 ton steel ingot

2012 IOP Conf. Ser.: Mater. Sci. Eng. 33 012091

(http://iopscience.iop.org/1757-899X/33/1/012091)

Modelling macrosegregation in a 2.45 ton steel ingot

J Li[1,2], M Wu[1,2], A Ludwig[2], A Kharicha[2]

[1] Christian Doppler Lab for Adv. Process Simulation of Solidification and Melting,
[2] Chair of Simulation and Modelling of Metall. Processes, Univ. Leoben, Austria

E-mail: Jun.Li@unileoben.ac.at

Abstract. A three phase model for the mixed columnar-equiaxed solidification was proposed by the current authors [Wu and Ludwig 2006 *Metall. Mater. Trans*. **37A** 1613-31]. The main features of the mixed columnar-equiaxed solidification are considered: the growth of the columnar dendrite trunks from the ingot surface, the nucleation and growth of the equiaxed crystals, the sedimentation of the equiaxed crystals, the thermal and solutal buoyancy flow and its interactions with the growing crystals, the solute partitioning at the solid-liquid interface during solidification, the solute transport due to melt convection and equiaxed sedimentation, the mechanical interaction/impingement between columnar and equiaxed crystals and the columnar-to-equiaxed transition (CET). However, due to the model complexity and the limited computational capability the model has not yet applied to the large steel ingots of engineering scale. This paper is going to simulate a 2.45 ton big-end-up industry steel ingot, for which some experimental results were reported [Marburg 1926 *Iron Steel Inst*. **113** 39-176]. Here a simplified binary phase diagram for the steel (Fe-0.45 wt. %C) is considered. Comparison of the modelling results such as as-cast columnar and equiaxed zones, macrosegregation with the experimental results is made. Details about the formation sequence of the distinguished crystal zones and segregation patterns are analyzed.

1. Introduction

Macrosegregation is a very common and serious defect in large steel ingots. The typical segregation pattern in a steel ingot consists of a positive segregation in the top part, a cone-shape negative segregation in the bottom part, inverse segregation near the surface, V segregates along the centerline, and A-segregates in the columnar zone [3-4]. This inhomogeneity occurs due to a relative motion between the liquid and solid phase during solidification. It is understood that this relative motion can arise as a result of thermo-solutal convection, shrinkage-induced feeding flow, flotation and sedimentation of free moving grain, mechanical or electromagnetic stirring, flow induced by pore or gas bubble formation, deformation of the solid skeleton, and capillary force induced flow [5].

Since the first modeling attempt of Flemings and co-workers [6-7] many macrosegregation models were presented [8-11]. Gu and Beckermann [11] for the first time have applied a fully coupled, multicomponent solidification model with melt convection to a large industry-scale ingot ($1.016 \times 2.08 \times 2.819$ m^3), their simulation result showed a qualitative agreement with the positive segregation in the top region of the ingot. However, since the neglect of sedimentation of free equiaxed crystals they could not predict negative segregation at the bottom. Combeau and co-workers [12-13] presented a two phase (solid and liquid) model to study the influences of motion and morphology of equiaxed

grain on a 3.3 ton big steel ingot. Some progress was made regarding to prediction of the bottom negative segregation zone, and the results have a good agreement with the experiment. Additionally, some streak-like segregates (A-segregates) were predicted.

The current authors [1, 14] for the first time developed a mixed columnar-equiaxed model which accounts directly for the nucleation and growth of the equiaxed globular grains, the growth of columnar dendrite trunks, and the effect of equiaxed grain sedimentation and melt convection. Their previous studies have successfully predicted both the cone negative segregation in the bottom region of ingot, and the columnar-to-equiaxed-transition (CET). However, due to the model complexity and the limited computational capability the previous studies were just based on the laboratorial scale of steel ingot. In this article, the mixed columnar-equiaxed is employed to study the macrosegregation in the industry-scale steel ingot on the base of the classic experiment [2].

2. Cast ingot: experiment and model description

Many industry-scale steel ingots were poured and analyzed for the segregation in the last century [2, 15]. As an example the sulphur print of a 2.45 ton big-end-up ingot (Fe-0.45 wt.%C) is shown in Figure 1(a). The nominal mixture concentration distribution ($(c_{mix}-c_0)/c_0$) is shown in Figure 1(b). As reference, this ingot is numerically studied. Configuration of this reference ingot, together with necessary boundary and initial conditions, is described in Figure 1 (c). Since the experiment was done many decades ago, due to the lack of precise process description, some process parameters and boundary conditions have to be derived on the base of assumptions. 2D axis symmetrical simulations are performed. Two cases are considered: Case I – using the mixed columnar-equiaxed three phase model; Case II – using the same model with the ignorance of the occurrence of equiaxed crystal. Table 1 lists some thermo-dynamic and physical properties.

Table1. Thermo-dynamic & physical properties[12]

Property	Units	Quantity
Melting of pure iron	K	1805.15
Liquidus slope	K (wt.%)$^{-1}$	-80.45
Equilibrium partition coefficient	-	0.36
Reference density	kg·m^3	6990
Specific heat	J kg^{-1} K^{-1}	500
Thermal conductivity	W m^{-1} K^{-1}	34.0
Latent heat	J kg^{-1}	2.71×10^5
Viscosity	Kg m^{-1} s^{-1}	4.2×10^{-3}
Thermal expansion coefficient	K^{-1}	1.07×10^{-4}
Solutal expansion coefficient	wt.%$^{-1}$	1.4×10^{-2}
Second dendritic arm spacing	m	5×10^{-4}
Diffusion coefficient (liquid)	m^2 s^{-1}	2.0×10^{-8}
Diffusion coefficient (solid)	m^2 s^{-1}	1.0×10^{-9}

Details of the numerical model are described elsewhere [1, 5, 14]. A brief outline of the model and simulation settings are given below:

- A simple boundary condition is applied. Here, the value of heat transfer coefficient is taken based on the final solidification time which refers to the classical theory and experiment ones [15].
- Three phases are defined: the primary liquid phase (ℓ), the equiaxed phase (e), and the columnar phase (c). The corresponding phase fraction is f_ℓ, f_e, and f_c with $f_\ell + f_e + f_c = 1$. Both the liquid and equiaxed phases are moving phases, for which the corresponding Navier-Stokes equations are solved. The columnar phase is assumed to stick to the wall, and solidifies from the wall towards the bulk melt. Thus, no momentum equation for the columnar phase is considered.
- Columnar dendrites are approximated by growing cylinders starting from the mould wall towards the casting centre. The advance of the columnar tip front was tracked during the solidification.

- Equiaxed grains are approximated as spheres. However, for the calculation of drag force the morphology of the equiaxed grains was modified as octahedral.
- A three-parameter heterogeneous nucleation law is used for the nucleation of equiaxed grains. No fragmentation and grain attachment are currently considered.
- Growth of the columnar trunk and equiaxed grain is governed by diffusion. Back diffusion is also considered.
- The permeability in the columnar mush zone is modelled according to Blake-Kozeny, while the drag law between the melt and equiaxed phase is modelled according to Wang's approach [16].
- Growth of columnar primary tips is stopped when the volume fraction of equiaxed phase in front of them reaches 0.49 (hard blocking criterion) [17].
- Packing limit for the equiaxed phase is set as $f_e + f_c \geq 0.637$ [18], and the equiaxed crystals are trapped when the trapping limit of $f_c \geq 0.2$ is reached [19].

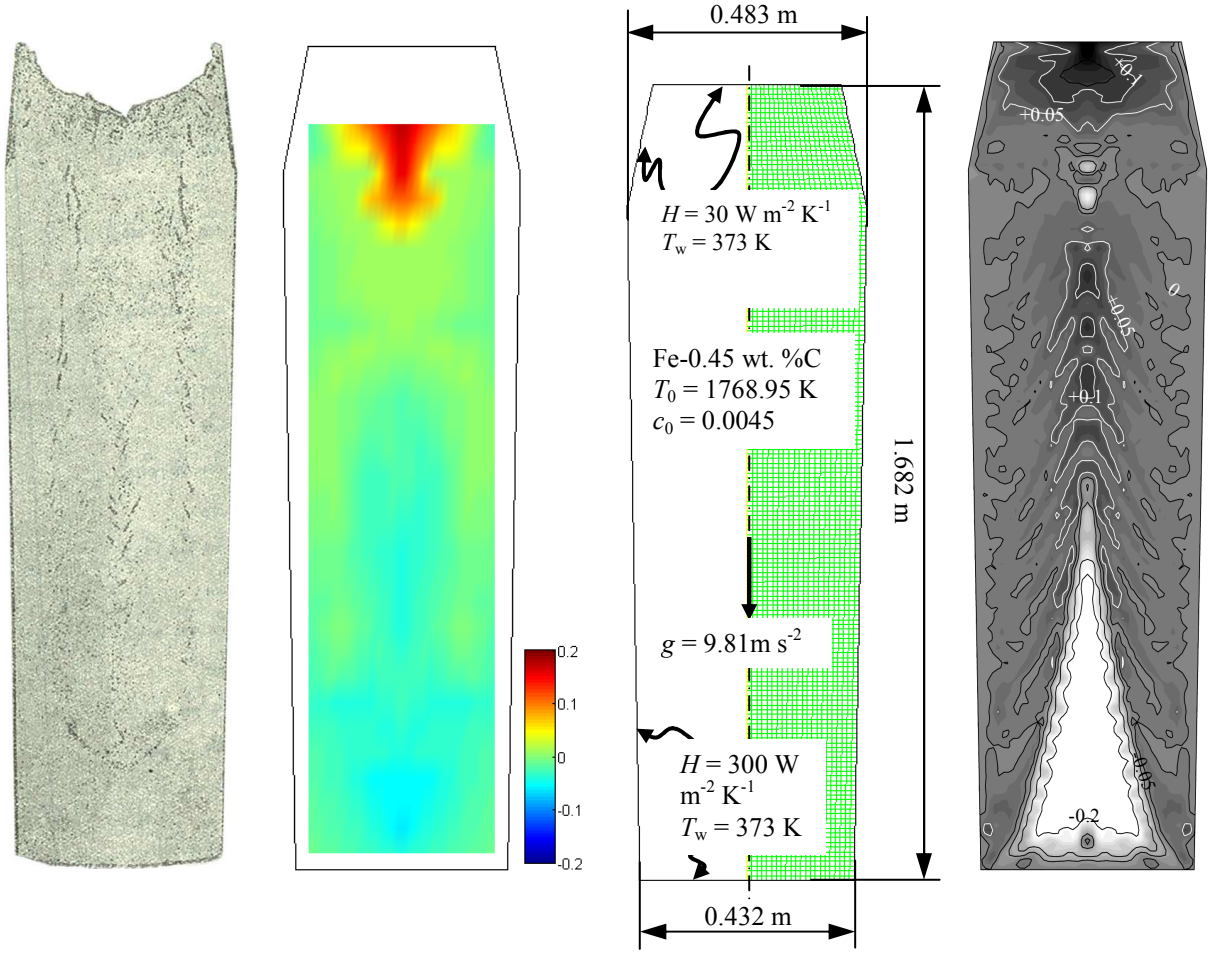

(a) sulphur print (b) measured segregation (c) simulation configuration (d) simulated segregation

Figure 1. Configuration of a 2.45-ton industry-scale steel ingot. (a)-(b) experiment [2], (c) simulation configuration and (d) simulated macrosegregation in grey scale (black for the positive segregation and light for the negative segregation) overlapped with isolines. The macrosegregation, both experimental (b) and simulated (d), is shown for the nominal mixture concentration $((c_{mix}-c_o)/c_o)$.

3. Simulation results and discussions

3.1. Case I: mixed columnar-equiaxed solidification

In this case full three phases are considered. The nucleation parameters for the equiaxed grains are assumed: n_{max} = 5×10^9 m^{-3}, ΔT_σ = 2 K, ΔT_N = 5 K. The simulated dynamic evolution of equiaxed grain volume fraction, columnar volume fraction, equiaxed grain sedimentation velocity and melt velocity at 100 s, 500 s, 1500 s, and 4000 s are shown in Figures 2(a) through (d), respectively. The final macrosegregation pattern is shown in Figure 1(d).

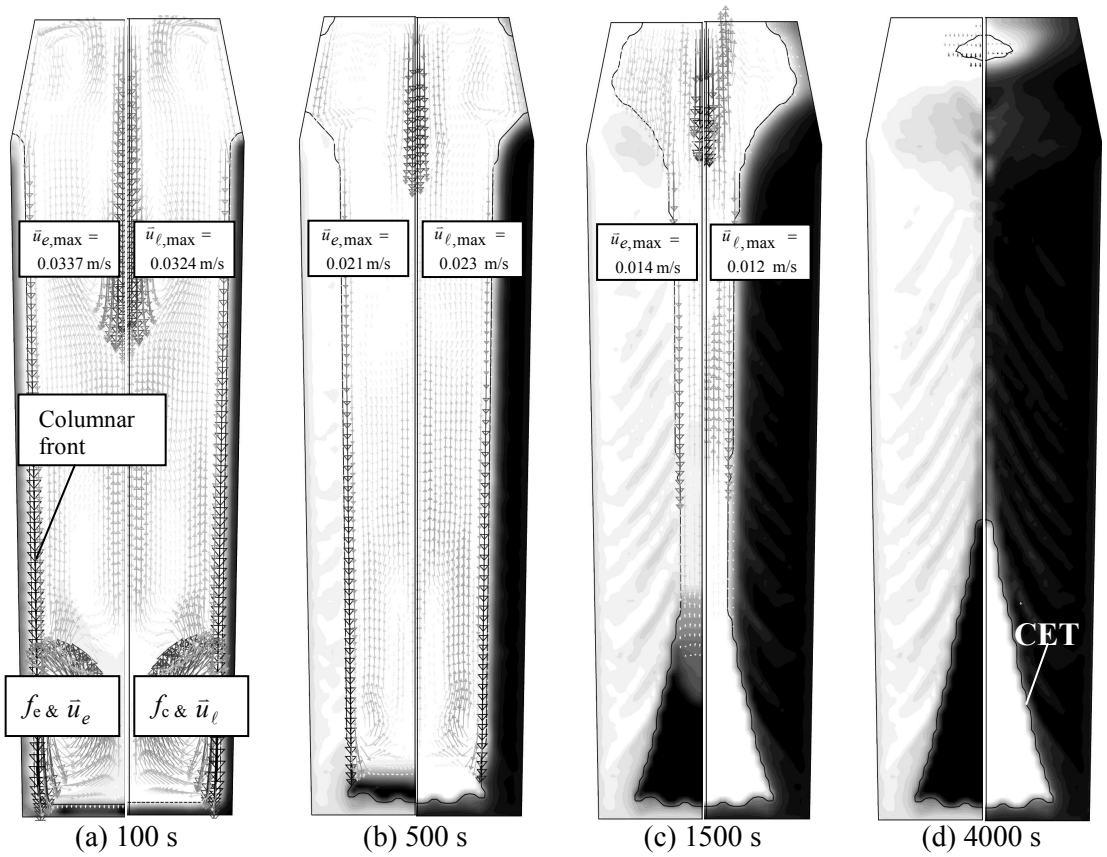

Figure 2. Solidification sequence of flow fields. The volume fraction of each phase (f_e or f_c) is shown in gray scale from 0 (bright) to 1 (dark). The left half of each figure shows the evolution of equiaxed volume fraction (f_e) together with the equiaxed sedimentation velocity ($\bar{u}_e$) in black arrows. The right half of each figure shows the evolution of columnar volume fraction (f_c) together with the melt velocity ($\bar{u}_\ell$) in black arrows. The columnar dendrite tip position also marked with a black solid line.

In the early stage of solidification, the equiaxed grains nucleate and grow gradually near the mould walls and bulk melt. Since the density of equiaxed grains are bigger than the melt, the equiaxed grains sink from the upper region to the bottom region, as shown in Figure 2(a). However, one may notice that in the centre part of the ingot there are some differences. In some regions the equiaxed sedimentation velocity is upward. Because the equiaxed volume fraction in these regions is very small (i.e. the momentum is small), the equiaxed grain sedimentation velocity is easily influenced and finally dominated by the upward liquid melt flow.

The direction of the liquid melt velocity near the columnar front is contributed by three factors: the solutal buoyancy force which will lead to the upward melt flow; the thermal buoyancy force which will lead to the downward melt flow; and the equiaxed sedimentation velocity which will drag the

surrounding melt flow downwards. It is clearly seen from the liquid melt flow field, which shows the downward melt flow there, that in this ingot the two downward factors are the decisive. The melt velocity direction near the columnar front is downward, however, due to the big scale of the ingot the melt velocity direction in the centre region is obscure and disorder.

As the sinking of the equiaxed grains leads to an accumulation of equiaxed grains in the bottom region of the ingot, the equiaxed grain density in the bottom region is bigger than the other regions which will increase the equiaxed solidification rate in this bottom region. As shown in Figure 2, the increasing of equiaxed volume fraction in the bottom region is faster than that in the other regions. This kind of sinking and accumulation of equiaxed grain will form a characteristic cone-shape distribution of equiaxed fraction in the bottom region.

As the columnar tip front is explicitly tracked, the simulation shows that the columnar tip fronts from both sides tend to meet in the ingot centre. However, in the lower part of the ingot the large amount of equiaxed grains stop the propagation of the columnar tip front. The final position of columnar tip indicates the columnar-to-equiaxed transition (CET) position. The CET separates the areas where only equiaxed grains appear from the areas where both columnar dendrites and equiaxed grains coexist. The CET line is predicted in this study, as seen in Figure 2(d). In addition, due to the disorder of both the sedimentation velocity and the melt convection, the sawtooth-like distribution of both the equiaxed phase and columnar phase volume fraction was found in the ingot. These sawtooth like profiles of both equiaxed phase and columnar phase volume fraction will definitely effect the final macrosegregation distribution.

Figure 1(d), presents the predicted final macrosegregation distribution. The cone-shaped negative segregation in the bottom region and a positive segregation zone in the upper region are obviously shown. The main mechanism for this cone-shaped negative segregation zone is grain sedimentation [5]. The settling grains were poor in solute and thus their pile-up results in a negative segregation at the bottom of the ingot. A further contributing factor to the strength of this negative segregation comes from the flow divergence of the residual liquid through this zone at a late solidification stage. The positive segregation in the upper region of the ingot is caused by the flow of the enriched melt in the bulk region. The solidification pattern agrees with the classical explanation of steel ingot solidification, summarized by Campbell [20].

One interesting result is detected that some streak-like patches of positive segregation were predicted near the mould wall and even in the centre region. These streak-like patches are somehow looks like the so called A-segregation [21]. Here we call these streak-like segregation as quasi-A-segregation. Most people consider that the main formation mechanism for A-segregation is: the flow disturbance in the mushy zone which will result in the flow channel and subsequently A segregation. The current authors [22-23] have studied the mechanism of channel segregation in a Sn-Pb benchmark. They denoted that the formation of channel segregation should be considered in two steps: (1) the initiation of channel, which is determined by the Rayleigh number; (2) the growth of channel which is the result of flow-solidification interactions. However, the formation mechanism of quasi-A-segregation in the current ingot must be different. In the early Sn-Pb benchmark the only driving force for the melt flow is thermal-solutal buoyancy force, whereas, in the current case the sedimentation of equiaxed grains and their inteactions with the columnar tip front and melt flow seem to play dominant role. The details about the mechanism for this kind of A-segregation are still to be investigated.

3.2. Case II: two-phase columnar solidification

Here, Case II used the same model and the same parameter as Case I. The only difference in this case is that we did not take into account the nucleation and growth of equiaxed grains. The solidification sequences and evolution of macrosegregation in two-phase columnar model are shown in Figure 3(a)-(c). The columnar tip front and volume fraction of columnar phase move from the mould walls towards the bulk melt region. For the solute-enriched interdendritic melt near the solidification front,

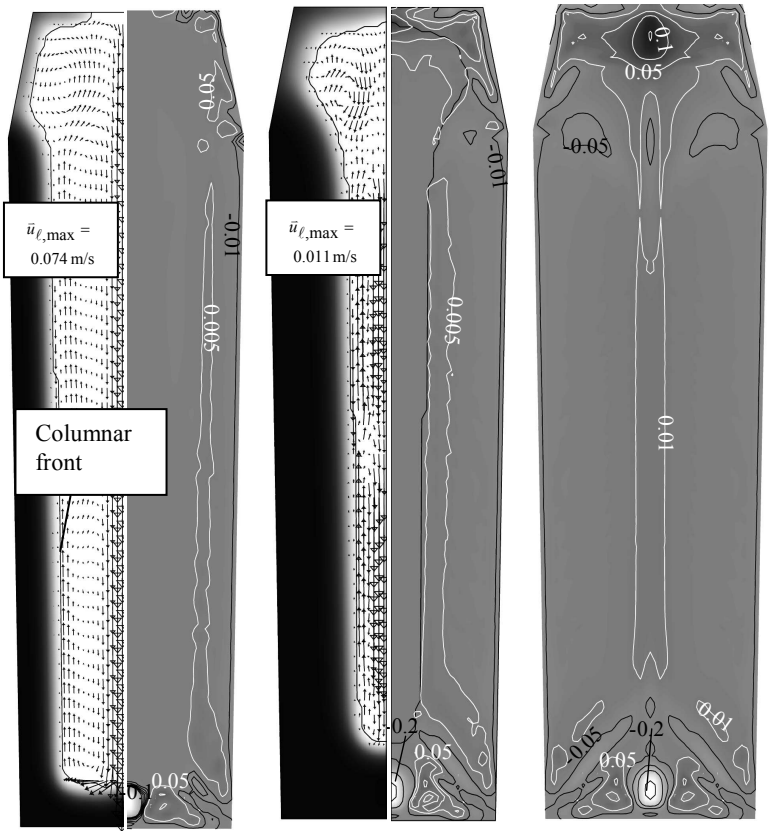

(a) 500 s (b) 1200 s (c) 3000 s

Figure 3. Solidification sequence and evolution of macrosegregation in the case of two-phase columnar solidification. In the left half of each figure the columnar volume fraction (f_c) is shown in gray scale together with the melt velocity ($\vec{u}_\ell$) in black arrows. In the right half of each figure the distribution of macrosegregation (((c_{mix}-c_o)/c_o) is shown in gray scale overlaid with macrosegregation iso-lines in solid lines. The columnar tip position was also indicated with a black solid line. Figure (c) shows the final macrosegregation distribution.

the solutal buoyancy leads to an upward flow. However, the thermal buoyancy leads to a downward flow. In this simulation case (Fe-0.45 wt. %C) the solutal buoyancy dominates over the thermal buoyancy, therefore the upward flow in the solidification front is the primary phenomena leading to the flow, as seen in Figure 3(a). The melt convection in the solidification front is upward, and this upward flow will drive the centre bulk melt to downward. Since the melt domain is large, the melt convection in the inside of bulk melt is disorder.

As seen from the final macrosegregation pattern in Figure 3(c), in the near wall region, where the solidification start from, a small degree of negative macrosegregation (-0.005) is predicted, while in the centre region, where the solidification is later on, a small degree of positive macrosegregation (0.01) is predicted. It is noted that a small region negative macrosegregation (relative macrosegregation value equal to -0.2) is found in the bottom region. In the upper region a positive macrosegregation is predicted with a relative macrosegregation value of 0.12. The reason for the negative segregation in the bottom middle region and the positive segregation in the upper middle region can be explained [5]: In the bottom middle region, since the solute enriched melt are replaced by the solute poor melt, the negative segregation tend to formation. The reason for the positive segregation in the upper middle region is that the solute poor melt is replaced by the solute enriched interdendritic melt from the solidification front.

4. Verification and discussions

The centre line segregation distributions are compared between the experiment results and the simulation results, as shown in Figure 4. The experiment shows the negative segregation in the lower part region and positive segregation in the upper region. The mixed columnar-equiaxed three-phase model also shows the negative segregation in the lower part and positive segregation in the upper part. However, the negative segregation in the lower part is predicted more seriously than the experiment result, and in the middle of upper part where the mixed three-phase model predicted the negative segregation while the experiment shows the positive segregation. The two-phase columnar

solidification case predicts a negative segregation in the bottom region and a small degree negative segregation in the middle of upper middle region. However, this model predicts a small degree positive segregation in the upper part region where both the experiment and the mixed three-phase model shown the negative segregation.

The possible explanation for the overestimate of the negative segregation in the lower part by the mixed columnar-equiaxed model could be in two aspects. On one hand, the assumption of totally spherical equiaxed grain will underestimate the average concentration for each equiaxed grain which subsequently will overestimate the serious of negative segregation in the bottom equiaxed zone. On the other hand, the overestimation of equiaxed nucleation in the whole ingot will also result in the overestimation of the negative segregation.

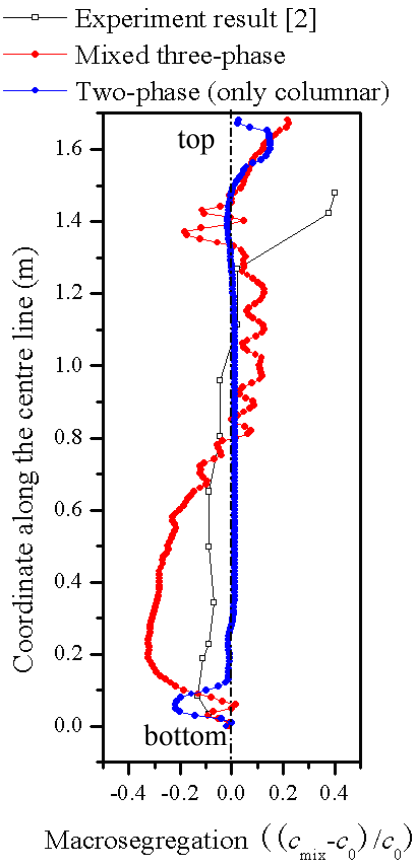

Figure 4. Comparison of macrosegregation ($((c_{mix}-c_o)/c_o)$) distribution along the centre of cast

As been observed from the lower part of the ingot, the mixed three-phase model (with the sedimentation of the equiaxed grain) overestimates the negative segregation. However, the two-phase columnar solidification case underestimates the negative segregation. Therefore, one possible conjecture is as follows: in this experiment there should contain a certain number of equiaxed grains in the lower part; this mixed three-phase model has overestimated the nucleation of equiaxed grain.

In the middle of the upper part, although the experiment shows the positive segregation, both of the simulation models predict the negative segregation. The reason for this deviation may also be in two aspects. Firstly, for the simulation case, during the final stage of solidification in the middle region of the ingot, the columnar tips will grow to the centre which will lead to the bridging and mini-ingotism in the upper part [24]. As the same mechanism as it forms in the whole steel ingot, eventually, the negative segregation will form in the middle of upper part. The second aspect is due to the ignorance of solidification shrinkage. In addition, as seen from the experiment curve, the distance between two points is in the order at least of 10 cm. It is known that in the region below the hot-topping and in the hot top part strong variations can occur. It means that the measured points did not provide sufficient resolution. People often found the negative segregation in the middle of upper part regions as well [12].

One should emphasize that the main purpose of this study is to show and verify that this mixed columnar-equiaxed model can be applied in the industry scale steel ingot, and can predict some reasonable macrosegregation patterns. We are not going to adjust some of the calculation parameters to cater for the experiment results. Since the experiments were done in many decades ago and many of the process parameters and material properties are unknown, the simulation results could only reproduce the experiment results in a qualitative manner.

5. Summary

A mixed columnar-equiaxed solidification model was applied to study the formation of macrosegregation in a 2.45 ton industry-scale steel ingot. It is verified that the experimentally reported segregation phenomena can be numerically simulated. The cone-shape negative segregation in the

bottom region and a positive segregation in the upper region of the ingot were predicted. The CET line, separating the purely equiaxed zone from the coexisting columnar-equiaxed zone, was predicted. The quasi-A-segregates near the mold wall were also found. The global macrosegregation distribution agreed qualitatively with the experimental result. However, the quantitative error of the numerical simulation is still quite large due to the lack of reliable process parameters and nucleation (equiaxed) parameters. The above-mentioned simulation was based on the assumed nucleation parameters ($n_{\max}$ = 5×10^9 m^{-3}, ΔT_σ = 2 K, ΔT_N = 5 K) for the equiaxed grains. One more simulation was performed with ignorance of the occurrence of equiaxed crystal. It is interesting to found that the latter case has a better quantitative agreement with the experimental result along the casting centerline than the former case with full three phases. It implies that the assumed nucleation parameters for equiaxed crystal in the former case have overestimated the amount of equiaxed grains, or the current 2.45 ton ingot might solidify mostly with columnar morphology. This hypothesis needs further verification.

Acknowledgments

The authors acknowledge the financial support by the Austrian Federal Ministry of Economy, Family and Youth and the National Foundation for Research, Technology and Development. Jun Li would like to thank the support from the China Scholarship Council.

References

[1] Wu M and Ludwig A 2006 *Metall. Mater. Trans.* **37A** 1613-31
[2] Marburg E 1926 *J. Iron steel Inst.* **113** 39-176
[3] Hultgren A 1973 *Scand. J. Met.* **2** 217-27
[4] Flemings M C 1976 *Scand. J. Met.* **5** 1-15
[5] Wu M, Könözsy L, Ludwig A, Schützenhöfer W and Tanzer R 2008 *Steel Res. Int.* **79** 56-63
[6] Mehrabian R and Flemings M C 1970 *Metall. Trans.* **1** 455-64
[7] Fujii T, Poirier D R and Flemings M C 1979 *Metall. Trans. B* **10B** 331-39
[8] Vannier H, Combeau H, Chevrier J C and Lesoult G 1991 *in Modeling of casting, welding and advanced solidification process V, TMS* (Warrendale, PA) 189-95
[9] Ohnaka I 1986 *in state of the art of computer simulation of casting and solidification processm* editor Fredriksson H, Les éditons de physique, Les Ulis, France 211-23
[10] Schneider M C and Beckermann C 1995 *Metall. Mater. Trans. A*. **26A** 2373-87
[11] Gu J P and Beckermann C 1999 *Metall. Mater. Trans. A.* **30A** 1357-66
[12] Combeau H, Založnik M, Hans S and Richy P E 2009 *Metall. Meter. Trans. B* **40B** 289-304
[13] Založnik M and Combeau H 2010 *Int. J. Therm. Sci*. **49** 1500-09
[14] Wu M and Ludwig A 2007 *Metall. Meter. Trans. A* **38A** 1465-75
[15] Marburg E 1953 *Trans. AIME* **5** 157-72
[16] Wang C and Beckermann C 1995 *Metall. Meter. Trans. B* **26B** 111-9
[17] Hunt J D 1984 *Mater. Sci. Eng*. **65** 75-83
[18] Wu M and Ludwig A 2009 *Acta Mater.* **57** 5621-31
[19] Ludwig A and Wu A 2005 *Mater. Sci. Eng.* A **413-414** 109-14
[20] Campbell J 1991 *Castings, Butterworth Heinemann Ltd*, Oxford
[21] Moore J J and Shah N A 1983 *Inter. Metals Reviews* **28** 338-56
[22] Li J, Wu M, Hao J and Ludwig A 2012 *Comp. Mater. Sci.* **55** 407-18
[23] Li J, Wu M, Hao J, Kharicha A and Ludwig A 2012 *Comp. Mater. Sci.* **55** 419-29
[24] Moore J J *Iron & Steel Soc.* 1984 **3** 11-20